

Tuning of metal-insulator transition of two-dimensional electrons at parylene/SrTiO₃ interface by electric field

H. Nakamura,^{1,2} H. Tomita,^{1,2} H. Akimoto,³ R. Matsumura,¹ I. H. Inoue,² T. Hasegawa,² K. Kono,³ Y. Tokura,^{2,4} and H. Takagi^{1,2,3}

¹*Department of Advanced Materials, University of Tokyo, Kashiwa 277-8561, Japan.*

²*Correlated Electron Research Center (CERC),
National Institute of Advanced Industrial Science and Technology (AIST),
AIST Tsukuba Central 4, Tsukuba 305-8562, Japan*

³*Advanced Science Institute, RIKEN (The Institute of Physical and Chemical Research), Wako 351-0198, Japan*

⁴*Department of Applied Physics, University of Tokyo, Tokyo 113-8656, Japan*

(Dated: April 30, 2021)

Electrostatic carrier doping using a field-effect-transistor structure is an intriguing approach to explore electronic phases by critical control of carrier concentration [1, 2]. We demonstrate the reversible control of the insulator-metal transition (IMT) in a two dimensional (2D) electron gas at the interface of insulating SrTiO₃ single crystals. Superconductivity was observed in a limited number of devices doped far beyond the IMT, which may imply the presence of 2D metal-superconductor transition. This realization of a two-dimensional metallic state on the most widely-used perovskite oxide is the best manifestation of the potential of oxide electronics.

The perovskite SrTiO₃ is sometimes called the “silicon of oxide electronics” because it is commonly used as a substrate for epitaxial growth of a variety of oxide films [3]. Not only it is an insulator with a band gap of 3.2 eV but also a quantum paraelectric with an extremely large dielectric constant of more than 10⁶ at low temperatures [4]. N-type conduction has been realized by introducing a small number of oxygen vacancies or by cation substitutions. An insulator to metal transition occurs at a rather low carrier concentration of $n \sim 10^{18} \text{ cm}^{-3}$ [5, 6] for a doped oxide system, which owes largely to the high mobility exceeding 10⁴ cm²/Vs. Superconductivity emerges in a limited concentration range from $n = 7 \times 10^{18}$ to $5 \times 10^{20} \text{ cm}^{-3}$ and the transition temperature T_c shows a bell shaped dependence on n with an optimum $T_c \sim 0.35 \text{ K}$ at $n \sim 10^{20} \text{ cm}^{-3}$ [7]. The carrier concentration required to achieve superconductivity is two orders of magnitude smaller than that for high- T_c cuprates which is a great advantage to realize electrostatic control of insulator-metal and superconductor transitions.

Such a unique doping properties of SrTiO₃ has triggered attempts to dope charged carriers electrostatically by using a field effect transistor (FET) structure. However, so far, attempts to realize metallic state have been unsuccessful [8]. This is due to several reasons, notably carrier trapping at the gate insulator/SrTiO₃ interface, Schottky barrier formation between SrTiO₃ and source and drain electrodes, and insufficient breakdown voltage of the gate insulators. An alternative approach has shown that two dimensional electron gas can be created at SrTiO₃/LaAlO₃ hetero-interface by a charge-transfer due to a polar discontinuity [9, 10, 11, 12, 13, 14] or possible oxygen defects [15]. This electronically tailored interface was found to be superconducting as in the bulk material [14].

Recently the performance of SrTiO₃ FET has been

drastically improved [16, 17] by overcoming the contacts and interface problems. These new devices showed metallic behavior down to 7 K [17]. In this Letter, we extend our study to lower temperatures below 1 K, and show that the two-dimensional insulator-metal transition is indeed achieved at the interface between parylene and SrTiO₃ reversibly while sweeping the gate voltage. A superconducting transition to zero-resistance state was observed at 0.13 K only in a sample where a large enough number of carriers were successfully introduced beyond the critical carrier number for the insulator-metal transition (IMT). The observation of two dimensional insulator-metal-superconductor transition represents major progress not only in the attempts for future oxide electronics but also in oxide physics.

A top gate FET was fabricated consisting of Au/parylene/SrTiO₃ layers. Al electrodes of the Hall bar geometry (Fig.1a) were evaporated on an atomically flat surface of SrTiO₃ (100) before depositing the gate insulator parylene. The use of Al electrode is the key to suppressing Schottky barrier formation. Details of the device fabrication are described elsewhere [17]. We have measured six samples (Sample A-F) with different parylene thickness (0.53-0.63 μm), corresponding to capacitance $C_i = 4.4 - 5.3 \text{ nF/cm}^2$ allowing a wide-ranging threshold gate voltage ($V_{th} = 97-170 \text{ V}$). Resistivity measurements above 2 K were carried out by dc four-probe method with temperature control by the Quantum Design Physical Property Measurement System, while those below 1 K were carried out by ac four-probe method (frequency 45 Hz) in a dilution refrigerator.

Figure 1a shows the temperature dependence of sheet resistance for various gate voltages (or electron densities). As the gate voltage is increased, the temperature dependence changes from insulating to metallic. At high enough gate voltages, the resistance eventually becomes metallic all the way down to a low tempera-

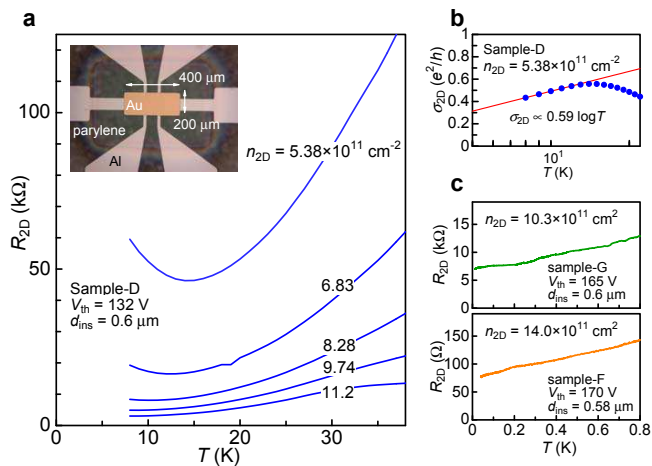


FIG. 1: Electrostatic control of metal-insulator transition of non-doped SrTiO₃ single crystal. (a) Temperature dependence of the sheet resistance (R_{2D}) tuned by the gate voltage near the metal-insulator transition. The parylene gate insulator thickness (d_{ins}) was 0.6 μm . Sheet carrier density (n_{2D}) in units of 10^{11} cm^{-2} is shown. n_{2D} is derived from the gate voltage V_G , capacitance C_i of parylene, and threshold gate voltage V_{th} ($n_{2D} = C_i(V_G - V_{\text{th}})/e$). The inset shows an photograph of sample with Al electrodes, parylene, and Au gate electrode. Channel area is $400 \mu\text{m} \times 200 \mu\text{m}$. (b) Sheet conductance in units of e^2/h plotted against $\log T$. (c) Sheet resistance versus temperature at $T < 1 \text{ K}$ in the case of $R_{2D} \ll h/e^2$. Metallic behavior ($dR/dT > 0$) is seen down to the base temperature (15 mK).

ture. The sheet carrier density (n_{2D}) here is estimated as $C_i(V - V_{\text{th}})/e$, where C_i is the capacitance per unit area. The sheet carrier density (n_{2D}) at the insulator to metal transition is approximately $1 \times 10^{12} \text{ cm}^{-2}$, which corresponds to a Fermi energy of about 1 meV assuming that the system is a two-dimensional (2D) free-electron gas. We also note that the sheet resistance (R_{2D}) in this regime is close to the two dimensional quantum sheet resistance $h/e^2 = 25.8 \text{ k}\Omega$. In the insulating state, R_{2D} shows logarithmic temperature dependence at lower temperatures as shown in Fig. 1b, and the slope is of the order of the quantum conductance. At first glance these observations suggest two-dimensional weak-localization [18, 19]. However, we show that the conduction in this weakly insulating regime is highly likely to be percolative in nature and not described by the weak localization scenario.

The above behavior suggests the emergence of 2D metal at the parylene/SrTiO₃ interface. This is in contrast to the scaling theory of localization, which predicts that a 2D system should become insulating at zero temperature [20]. Recent experiments on very high mobility 2D electron gases formed in Si and GaAs hetero-structure, however, demonstrated the existence of insulator-metal transitions even in 2D and have been attracting a considerable attention [21]. To explore the ground state of electrostatically induced metallic inter-

face between parylene and non-doped SrTiO₃ single crystal, we extend the transport measurements down to 15 mK using a dilution refrigerator for the samples with R_{2D} well below the quantum resistance. Figure 1c shows a typical result. The metallic behavior ($dR/dT > 0$) is observed down to $\sim 15 \text{ mK}$. As shown in Fig. 1a, when the gate voltage is reduced, R_{2D} shows an insulating ($dR/dT < 0$) behavior. We emphasize here that the two ground states can be tuned reversibly by the electrostatic control through the parylene gate insulator.

Compared to conventional semiconductors like Si or GaAs, SrTiO₃ has a large dielectric constant of the order of 10^6 at low temperatures [4] which weakens the confining potential at the interface. Therefore, it should be clarified whether or not the electronic state formed at parylene/SrTiO₃ interface is two-dimensional. We have checked this experimentally by measuring the anisotropy of transverse magnetoresistance $\Delta R/R_0$. Here, ΔR is the resistance change in a magnetic field and R_0 is the zero-field resistance. Figure 2 shows the magnetoresistance taken under B perpendicular to the plane, and parallel to the plane. The large positive magnetoresistance, indicative of a high mobility, is observed only for the field perpendicular to the plane. No appreciable magnetoresistance is seen for the field parallel to the plane, which implies that the thickness of the conducting layer is much thinner than the cyclotron radius of electrons, $r_c = \frac{m^* v_F}{eB} = \frac{\hbar k_F}{eB}$, (m^* ; the electron effective mass [25], v_F ; Fermi velocity, k_F ; Fermi wave number, $\hbar = h/2\pi$, where h is Planck's constant), which we estimate $r_c \sim 15 \text{ nm}$ at $B = 6 \text{ T}$. Numerical calculation based on the Schrödinger-Poisson equation with a triangular potential approximation estimates the conducting layer depth to be approximately 10 nm in metal/insulator/SrTiO₃ structure [22] and support the presence of two-dimensional electron system. It should also be noted that this estimation of conducting layer depth may become even smaller when the rapid decrease of dielectric constant of SrTiO₃ at large electric field is taken into account [23, 24]. From these results, we conclude that the metal-insulator transition observed in the parylene/SrTiO₃-FET is two-dimensional in nature.

Figure 3a shows the sheet resistance R_{2D} as a function of the sheet carrier density n_{2D} at 4.2 K. A notable feature of the electrostatically-induced IMT is the sharp and almost discontinuous decrease of the resistance with increasing the sheet carrier density. With further increasing the carrier density, a “kink” in R_{2D} - n_{2D} is clearly recognized, and above the kink, much more moderate decrease is observed, where metallic behavior of resistivity is seen down to the lowest temperature. The comparison of two kinds of mobilities deduced from the magnetoresistance and the field-effect, respectively, suggests phase separation into metallic and insulating domains in the transition region before reaching the kink, implying that the insulator to metal transition is very likely discontinuous. Figure 3b shows the evolution of carrier mobility near the transition, where

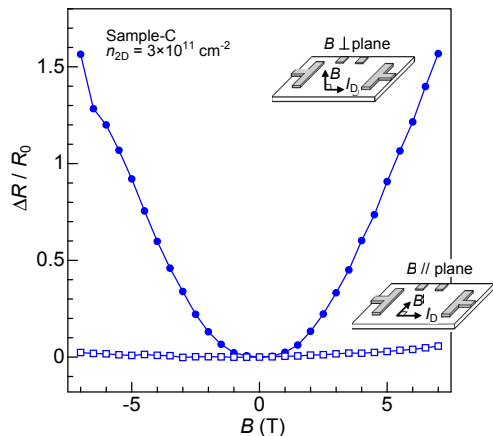


FIG. 2: Anisotropic magnetoresistance. Magnetoresistance $\Delta R/R_0$ for two different orientations of magnetic field B at 4.2K: perpendicular and parallel fields to the SrTiO₃/parlyene interface. Positive magnetoresistance for the perpendicular field is caused by the cyclotron motions of electrons and its magnitude is related to the mobility μ of the electron gas ($\Delta R/R_0 \sim (\mu B)^2$). Little effect for the parallel field indicates that the conducting layer is much thinner compared to the cyclotron radius of electrons.

two independent mobilities are compared; the field-effect mobility $\mu_{FE} = (1/e)(d\sigma_{2D}/dn_{2D})$, where $\sigma_{2D} = 1/R_{2D}$, $n_{2D} = C_i V_G/e$, and the magnetoresistance mobility μ_{MR} estimated by the magnitude of the quadratic part of magnetoresistance $\Delta R/R_0 = (\mu_{MR} B)^2$ [26]. While the two mobilities agree very well in the larger gate voltage region above the kink, they are distinct from each other in the transition region (Fig. 3b). The μ_{MR} is as large as 2000 cm²/Vs and surprisingly independent of carrier density above and below the kink. In contrast, μ_{FE} shows a rapid decrease with decreasing voltage around the transition region. This contrasting behavior between the two mobilities may be understood naturally in terms of phase separation. The conduction should be dominated by the metallic domains. The magnetoresistance is then almost identical to those of metallic domains independent of the gate voltage. On the other hand, the value of μ_{FE} reflects the channel resistance. Narrowing of the metallic domain during the separation enhances the channel resistance and hence μ_{FE} decreases rapidly. Thus, the transition between metallic and insulating state tuned by a gate voltage is very likely a first order transition accompanied by a phase separation. The origin of seemingly weak localization behavior in the transition region shown in Fig. 1 is not clear. We suspect that narrow percolation path in the mixed phase might be responsible for the apparent logarithmic temperature dependence.

The discontinuous transition presented here is reminiscent of the “steplike” change in conductance observed in SrTiO₃/LaAlO₃ hetero-structures as a function of LaAlO₃ thickness [11], where the electric field produced by polar discontinuity is believed to play a role. In both

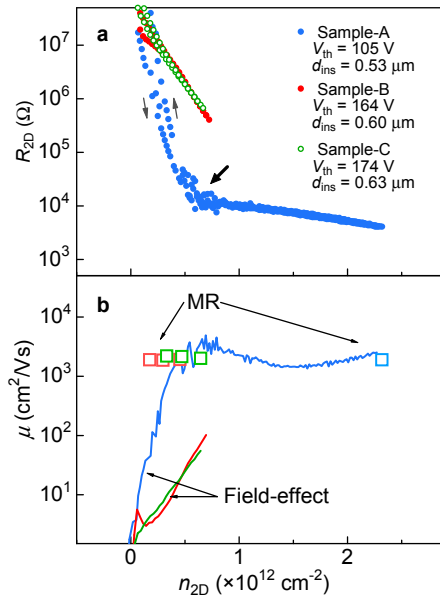


FIG. 3: Electrostatic tuning of the sheet resistance and the mobilities. (a) Sheet resistance R_{2D} plotted against the sheet carrier density n_{2D} at 4K. The position of a “kink” is shown by a thick arrow. (b) Field-effect mobility: $\mu_{FE} = (1/e)(d\sigma_{2D}/dn_{2D})$, and magnetoresistance mobility μ_{MR} : $\Delta R/R_0 = (\mu_{MR} B)^2$. Two mobilities show significant difference near the threshold of gate voltage (early stage after the accumulation of mobile charge), but coincide at large n_{2D} .

cases, the sheet resistance of the conducting side of the “discontinuous change” is of order 10 kOhm, suggesting there exists a universal minimum metallic conductivity of around $\sim 10^{-4}$ S. Although the mechanism of first-order-like metal-insulator transition is currently unclear, the observation of similar behavior in different types of device structure seems to indicate that the origin of discontinuous metalization may be intrinsic at least to SrTiO₃.

In only a few samples, we were able to apply a large enough gate voltage without breaking the gate insulator (parlyene) to go far beyond the discontinuous IMT. With successful accumulation of an enough number of carriers, we observed zero-resistance state associated with superconductivity. As shown in Fig. 4, at 128 mK the resistance decreases gradually with increasing gate voltage, namely the carrier concentration, and eventually becomes zero within our resolution above $n_{2D} \sim 2 \times 10^{12}$ cm⁻². With decreasing gate voltage, then, the resistance goes back to a finite value reproducibly. With increasing temperature from 128 mK at $n_{2D} \sim 2.2 \times 10^{12}$ cm⁻², the resistive transition to a normal state is observed around 130-160 mK as seen in the inset of Fig. 4. The application of magnetic field of 0.03 T perpendicular to the plane was found to suppress the zero resistance state.

These observations demonstrate that superconductivity is marginally achieved around $n_{2D} \sim 2 \times 10^{12}$ cm⁻².

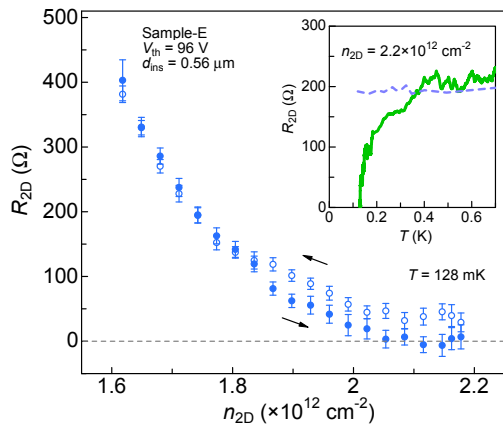


FIG. 4: Continuous and reversible electrostatic tuning of superconductivity at the surface of undoped SrTiO₃ single crystal. Reversible and continuous control between the zero-resistance and the finite resistance was achieved by sweeping the gate voltage at $T = 128$ mK. The inset shows temperature dependence of the sheet resistance at a constant sheet carrier density at $B = 0$ T (continuous line) and at $B = 0.03$ T (dashed line). Zero-resistance is seen below 130 mK for $B = 0$ T.

This sheet carrier density corresponds to $n_{3D} \sim 2 \times 10^{18} \text{ cm}^{-3}$ assuming the thickness of 2D electron layer to be 10 nm. Though the reason is not obvious, this is similar to the onset $n_{3D} \sim 7 \times 10^{18} \text{ cm}^{-3}$ reported for bulk, given the uncertainty in 2D electron layer thickness. Note that we did not see any trace of superconductivity in the metallic sample shown in Fig. 1c, down to 15 mK at $n_{2D} \sim 1 \times 10^{12} \text{ cm}^{-2}$. These suggest that the 2D insulator-metal transition occurs first and that, to

achieve 2D metal-superconductor transition, extra charge carrier must be introduced. We, however, cannot rule out completely superconductivity at an extremely low temperature in the sample near IMT.

It should be noted that by applying a large gate field for a long period (typically $V_G > 150$ V for one week), another superconductor-like transition without a zero resistance state appears around 0.35 K which does not disappear even after reducing the gate field. This is highly likely to be the superconductivity associated with the creation and/or migration of oxygen defects at the interface.

In conclusion, we have demonstrated that the parylene/SrTiO₃ interface shows a transition from an insulator into two-dimensional metal by the electrostatic carrier doping as observed in high mobility 2D electron gas formed in Si and GaAs hetero-structures. We believe that this represents a breakthrough in oxide electronics. One of the unique features of the parylene/SrTiO₃ interface is a zero-resistance state emerging at 130 mK. The emergent superconductivity is thought-provoking not only because of the possible 2D character but also because it develops in a electron gas with a small Fermi energy of a few meV—usually trivial interactions like spin-orbit coupling [27] can be comparable with Fermi energy in this system and may give rise to an exotic superconductivity. Therefore, what we have demonstrated in this study is not simply a hectic chase of oxide electronics after the conventional semiconductor but also a prologue to new paradigm of transition metal oxide physics.

We thank R. Perry for critical reading of the manuscript. This work was supported in part by MEXT, Grant-in Aid for Scientific Research (S)(19104008).

-
- [1] C. H. Ahn *et al.*, Rev. Mod. Phys. **78**, 1185 (2006).
[2] M. Imada, A. Fujimori and Y. Tokura, Rev. Mod. Phys. **70**, 1039 (1998).
[3] M. Kawasaki *et al.*, Science **266**, 1540 (1994).
[4] K. A. Müller and H. Burkard, Phys. Rev. B **19**, 3593 (1979).
[5] O. N. Tufte and P. W. Chapman, Phys. Rev. **155**, 796 (1967).
[6] H. P. R. Frederikse and W. R. Hosler, Phys. Rev. **161**, 822 (1967).
[7] C. S. Koonce, Marvin L. Cohen, J. F. Schooley, W. R. Hosler and E. R. Pfeiffer, Phys. Rev. **163**, 380 (1967).
[8] K. Ueno *et al.*, Appl. Phys. Lett. **83**, 1755 (2003).
[9] A. Ohtomo and H. Y. Hwang, Nature (London) **427**, 423 (2004).
[10] K. S. Takahashi *et al.*, Nature **441**, 195 (2006).
[11] S. Thiel, G. Hammerl, A. Schmehl, C. W. Schneider, and J. Mannhart, Science **313**, 1942 (2006).
[12] G. Herranz, *et al.*, Phys. Rev. Lett. **98**, 216803 (2007).
[13] A. Brinkman, *et al.*, Nature Materials **6**, 493 (2007).
[14] N. Reyren, *et al.*, Science **317**, 1196 (2007).
[15] J. L. Maurice *et al.*, Europhysics Letters **82**, 17003 (2008).
[16] K. Shibuya, *et al.*, Appl. Phys. Lett. **88**, 212116 (2006).
[17] H. Nakamura *et al.*, Appl. Phys. Lett. **89**, 133504 (2006).
[18] G. Bergmann, Phys. Rep. **107**, 1 (1984).
[19] Y. Kozuka, Y. Hikita, T. Susaki and H. Y. Hwang, Phys. Rev. B **76**, 085129 (2007).
[20] E. Abrahams, P. W. Anderson, D. C. Licciardello, and T. V. Ramakrishnan, Phys. Rev. Lett. **42**, 673 (1979).
[21] S. V. Kravchenko, and M. P. Sarachik, Rep. Prog. Phys. **67**, 1 (2004).
[22] I. H. Inoue, Semicond. Sci. Technol. **20**, S112 (2005).
[23] H.-M. Christen, J. Mannhart, E. J. Williams, and Ch. Gerber, Phys. Rev. B **49**, 12095 (1994).
[24] T. Susaki, Y. Kozuka, Y. Tateyama, and H. Y. Hwang, Phys. Rev. B **76**, 155110 (2007).
[25] H. Uwe, R. Yoshizaki, T. Sakudo, A. Izumi, and T. Uzunaki, Jpn. J. Appl. Phys. **Suppl.24-2**, 335 (1985).
[26] T. R. Jervis and E. F. Johnson, Solid-State Electron. **13**, 181 (1970).
[27] R. Winkler, *Spin-orbit coupling effects in two-dimensional electron and hole systems.*, (Springer, Berlin, 2003).